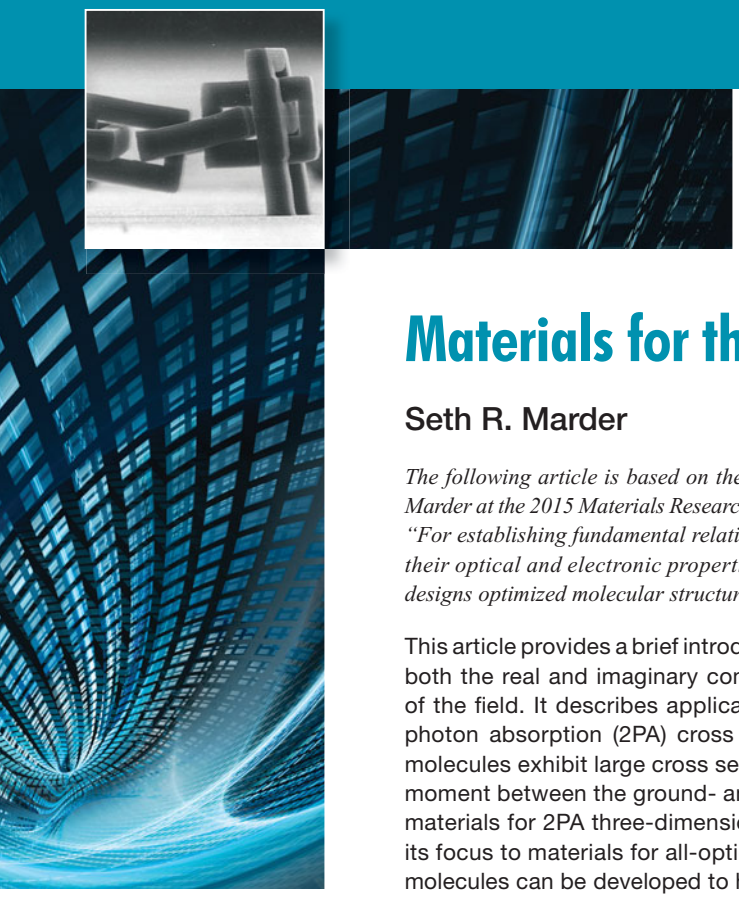


Materials for third-order nonlinear optics

Seth R. Marder

The following article is based on the MRS Mid-Career Researcher Award presentation given by Seth Marder at the 2015 Materials Research Society Spring Meeting in San Francisco. Marder was recognized "For establishing fundamental relationships between the chemical structure of organic molecules and their optical and electronic properties, thereby profoundly impacting how the scientific community designs optimized molecular structures for use in nonlinear optical applications."

This article provides a brief introduction to third-order nonlinear optical materials, including both the real and imaginary components, and is intended to be a personal perspective of the field. It describes applications that can be enabled by molecules with large two-photon absorption (2PA) cross sections and how symmetrical donor–(π-bridge)–donor molecules exhibit large cross sections associated with significant changes in quadrupole moment between the ground- and first-excited electronic states. The application of such materials for 2PA three-dimensional microfabrication is described. The article then turns its focus to materials for all-optical switching applications and explains how cyanine-like molecules can be developed to have both very large real third-order nonlinear coefficients and small 2PA cross sections, both of which are necessary for efficient all-optical switching materials.

Introduction

The application of an electric field to an atom induces polarization and an associated dipole moment. In an oscillating electric field, the electrons in a molecule also oscillate in response to the field. A plot of the induced dipole moment (polarization), μ induced, in a molecule as a function of the applied field will be linear if the molecule has a linear restoring force for the electrons around the nuclei. At the molecular level, an equation for this relationship is given by:

$$\mu_{\text{induced}} = \alpha E, \tag{1}$$

where E is the electric field, and α is the linear polarizability. At the material level, one can write an analogous equation for the polarization density, which is related to the electric field by the constant referred to as the first-order susceptibility $\chi^{(1)}$—this is also related to the dielectric constant, and therefore, is the square of the refractive index of a material.[1]

Not all materials respond linearly to an oscillating electric field. In some cases, there is a significant deviation from linearity in a plot of the induced dipole moment as a function of the electric field (especially at high field strengths), which can be described by expressing dipole moment as a Taylor series expansion as a function of the field (shown below to third order in the field):

$$\mu_{\text{induced}} = \alpha E + \beta/2\ E^2 + \gamma/6 E^3 + \ldots . \tag{2}$$

Beyond the first term, αE, the terms scale with higher powers of the field, for example, quadratically (β) and cubically (γ) with the electric field; these terms are referred to as "nonlinear polarization" terms.

Both β and γ ($\chi^{(2)}$), second-order susceptibility, and $\chi^{(3)}$, third-order susceptibility, for bulk materials, respectively) give rise to interesting effects that can be used, for example, for optical switching and for generation of new frequencies using lasers. In order to generate these effects and others efficiently, we are interested in understanding how to design molecules and materials that optimize molecular nonlinearity and bulk nonlinear susceptibility. In this article, we limit the discussion to effects that scale as the third-power of the electric field (E^3),[1–16] referred to as third-order nonlinear optical effects. The term that relates E^3 to the induced polarization on the molecular level is the "second-hyperpolarizability" (or "third-order polarizability") (γ), and on the bulk materials level is the "third-order susceptibility" ($\chi^{(3)}$).

Seth R. Marder, Georgia Institute of Technology, USA; seth.marder@chemistry.gatech.edu
DOI: 10.1557/mrs.2015.310

© 2016 Materials Research Society

https://doi.org/10.1557/mrs.2015.310 Published online by Cambridge University Press

There is both a real[1,6,10–15] and an imaginary part of $\chi^{(3)}$.[2–4,7–9] The real part, $\mathrm{Re}(\chi^{(3)})$ is the "nonlinear refractive index," which describes how the refractive index of a material changes in the presence of an electric field, for example, an intense light source such as that from a pulsed laser. The ability to modulate the refractive index of a material by an intense light beam enables the material to be utilized for a variety of optical-switching applications.

The imaginary part, $\mathrm{Im}(\chi^{(3)})$, is related to a process referred to as "two-photon absorption" (2PA), in which the molecules simultaneously absorb two photons of light to create an excited state whose energy lies at the sum of the energies of the two absorbed photons. Two-photon absorption gives rise to interesting phenomena. For materials exposed to an intense focused laser beam, excitation will be mainly confined in three dimensions at the focus of the laser beam. For certain applications, very strong 2PA arising from a large $\mathrm{Im}(\chi^{(3)})$ is desirable, and for other applications, a very large nonlinear refraction arising from a very large $\mathrm{Re}(\chi^{(3)})$ is desirable.

Additionally, in some cases where we want a very large $\mathrm{Re}(\chi^{(3)})$, having any 2PA (i.e., $\mathrm{Im}(\chi^{(3)}) > 0$) at the wavelength of interest is very detrimental. In some instances, we want to both maximize $|\mathrm{Re}(\chi^{(3)})|$ and minimize $\mathrm{Im}(\chi^{(3)})$. Fortunately, quantum chemists can help us describe the essence of third-order nonlinear optical effects with equations, derived from perturbation theory, that relate third-order nonlinearity to the transition moments, transition energies, and changes in dipole moments associated with optical transitions. Working in concert with quantum chemists, one can ask: How can quantum-chemical equations be translated into molecular structure–property relationships that can guide the design of materials with desired properties?[1]

Before delving into structure–property relationships, it is instructive to first briefly describe applications related to both the real and imaginary parts of $\chi^{(3)}$. For $\mathrm{Re}(\chi^{(3)})$, one can take advantage of the intensity-dependent refractive index of a material in such a way so as to enable all-optical switching applications (AOS), as described later in the text. Also, as mentioned previously, $\mathrm{Im}(\chi^{(3)})$ is responsible for 2PA, which has many applications. However, only those that take advantage of the spatial confinement of excitation near the focus of a laser beam will be discussed. Since we can precisely control where excitation of molecules in three dimensions takes place, there can be, for example, excitation of fluorescence at a very small spot and, consequently, three-dimensional (3D) imaging of fluorescence in materials and in living tissues without having to filter out nonfocal point fluorescence, such as in confocal microscopy.

One can also make 3D optical memory or fabricate 3D micrometer-sized structures where chemical (and physical) changes in the materials can be realized precisely in three dimensions by 2PA-induced processes.[3,5,9] Although 3D printing holds promise in additive manufacturing, 2PA allows for 3D microfabrication on a scale ca. 100× smaller than the lower size limits of conventional 3D printing. In the case of 2PA fabrication, truly nanoscopic structures (i.e., with feature sizes under 100 nm) can be created with 3D control using visible light as the excitation source by activating chemistry that changes the property of a material in a confined volume in three dimensions.

Two-photon absorbing materials and applications

My group's 2PA-focused research program—in collaboration with my colleague Joseph Perry—started nearly 20 years ago when we observed a very simple organic molecule with a "stilbene" (C_6H_5–CH=CH–C_6H_5) core shown in the top left of **Figure 1**. Donors on each end had a 2PA cross section that was ~20× that of stilbene itself (i.e., without donors on the end).[2] It was conjectured that the 20× increase in cross section was due to the fact that, upon excitation, there was a symmetrical redistribution of electron density from the donors on the ends of the molecule toward the middle that caused a change in quadrupole moment. Our long-time collaborator, Jean-Luc Brédas, performed extensive calculations on these molecules and was able to reproduce the 20× difference in cross section and confirm that indeed there was a large change in the quadrupole moment of these molecules upon excitation.[2]

Our team hypothesized that molecules could be designed to have even larger cross sections than that observed for the bis(donor)-substituted stilbene (which was one of the largest cross sections that had been reported for any organic molecule at the time). This could be achieved by increasing the length over which charge was transferred during excitation to increase the change in quadrupole moment or to increase the

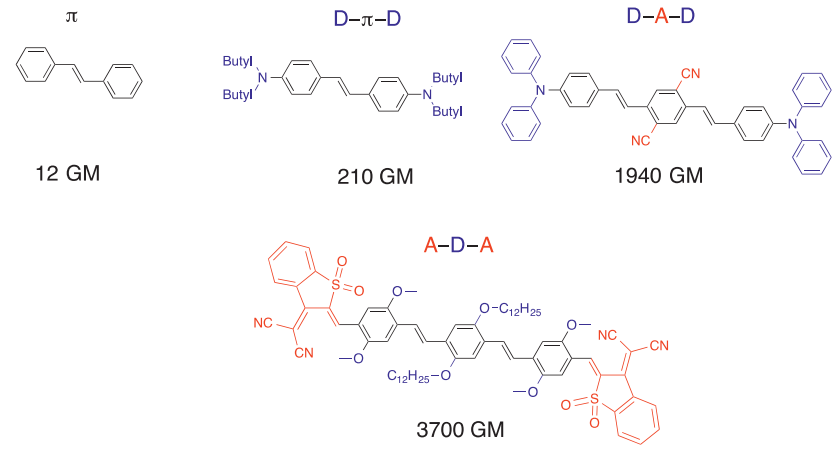


Figure 1. Examples of the effects of variation of chemical structure on two-photon absorption cross sections starting with stilbene (top left going clockwise) and showing the effects of adding donors to the end (D–π–D), acceptors to the middle (D–A–D), and the reverse (A–D–A). Note the enhancement of the cross section with increasing conjugation length (1 GM = 10^{-50} cm^4s/photon). Reproduced with permission from Reference 2. © 1998 American Association for the Advancement of Science; and Reference 4. © 2000 American Chemical Society.

https://doi.org/10.1557/mrs.2015.310 Published online by Cambridge University Press

amount of charge that was transferred, not only by having donors at the ends of the molecules, but also by having acceptors at the middle (or vice versa). Many examples of these types of molecules were synthesized in our labs. Perry's group characterized their cross sections, and Brédas' group performed extensive calculations to provide theoretical support. To summarize and simplify well over a decade of work, this simple design strategy is robust and has now been successfully applied to a large variety of organic structures by many groups around the world. Today, molecules have been identified that have cross sections on the order of 100–200× the cross section of the best molecules at that time (Figure 1).[2,4,7]

Many of the molecules that have large 2PA cross sections are fairly easily oxidized in the ground state by virtue of being substituted with strong donors, and, largely for the same reason, they are very strong excited-state reducing agents. As a consequence, these molecules can be used to initiate chemical reactions induced by an electron transfer reaction triggered by 2PA. For instance, one can transfer an electron to an acrylate group (CH_2=CH(CO_2R), R = alkyl group) and create an acrylate radical anion, which can then find a proton to create an acrylate radical, which then initiates radical chain polymerization.[3,8] If 2PA triggers the electron transfer event,[2,5] then, under the correct conditions, polymerization can be confined to a very small volume element (voxel) at the focus of the laser beam. (For reasons that are beyond the scope of this article, the polymerization can actually be confined to a size smaller than the diffraction limit of the laser beam.) If this is done using a monomer that has at least two acrylate groups, then the polymerization will create a cross-linked acrylate that often has enough mechanical integrity to produce defined structures. Since the laser beam can be moved in three dimensions and turned on and off, the buildup of complex 3D structures is relatively easily compared to lithographic techniques.

One of the initial structures fabricated in this manner in Perry's group is shown as an example in **Figure 2**.[8] Many of these initial structures are on a scale comparable to the thickness of a human hair (50 μm), which is rather large relative to what has subsequently been shown to be achievable. Photonic crystals, microfluidic structures, and surfaces to use as templates for tissue engineering can be created.[2] In addition to acrylate polymerization, it was also found that molecules that generate a proton upon 2PA can be designed; these are known as two-photon "photoacid generators" (PAGs).[5] They can be used to polymerize acid-sensitive monomers such as epoxides, or they can change materials that are insoluble in a particular solvent mixture to becoming soluble by breaking off functional groups. The 2PA PAGs made in our group have two-photon sensitivities (i.e., the product of the quantum yield of acid generation and the 2PA cross section) that are ca. 5–30× more sensitive than conventional PAGs used in the lithography industry. Consequently, using 2PA with our PAGs, researchers can write faster or write with much lower intensity and higher fidelity. Subsequent to our early publications, the field has taken off, and researchers around the world are now performing 3D microfabrication using 2PA. Anyone can search Google images for "two-photon 3D fabrication" and view an amazing assortment of images of microscale structures, including renditions of the Eiffel Tower, the Brandenburg Gate in Berlin, the Statue of Liberty, Tower Bridge in London, and the Empire State Building; replicas of insects; and microscale versions of some classical sculptures. It is important to note that most of these complex 3D objects can fit within the width of a human hair, which is not easy to achieve by techniques other than "two-photon 3D microfabrication"; for example, they cannot be made by conventional 3D printing at these length scales. It is gratifying that our team played a significant role in laying out the molecular design guidelines that helped to spark this intense technological development around the globe.

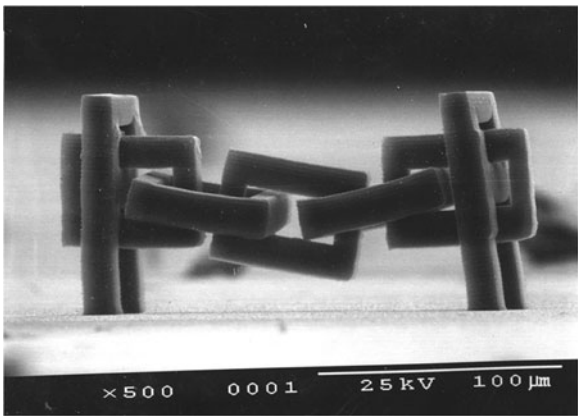


Figure 2. Example of a microstructure fabricated by two-photon three-dimensional microstructures based upon a crosslinkable acrylate.[8] Courtesy of Joseph Perry.

Materials with large |Re($\chi^{(3)}$)| for AOS applications

One of the main uses of the real part of the third-order nonlinear optical susceptibility is AOS. The quantity of information transferred monthly keeps increasing dramatically and is likely to keep increasing as users seek faster and more data transfers with the explosion of cloud computing. For the purpose of this article, we assert that using third-order nonlinear processes to switch optical signals with light can avoid the need to convert light signals to electrical signals and back into light signals during routing, thus increasing data speeds.

In order to perform efficient optical switching using third-order nonlinear processes, the index of refraction of a material needs to be modulated. Utilizing the real part of $\chi^{(3)}$, all-optical switching can be implemented in a variety of device architectures. For example, imagine splitting a light beam into two paths, or arms, and letting the light travel along each path before recombining the two beams; this is the basic structure of a device known as a Mach-Zehnder interferometer.[17,18] If the paths are of equal length through materials of identical refractive index, the two beams interfere constructively, and the original input signal is recovered. If, on the other hand, the paths

https://doi.org/10.1557/mrs.2015.310 Published online by Cambridge University Press

differ sufficiently in refractive index, the beams may interfere destructively. One of the beams will accumulate a phase shift relative to the other as it travels through an arm, and if the difference in the indices of refraction between the two arms is sufficiently large, the beam can accumulate a 180° phase shift before they recombine, resulting in complete destructive interference.

Using a Mach-Zehnder interferometer composed of $\chi^{(3)}$ materials, a control pulse of intense light applied to one arm of the interferometer can change the refractive index in that arm controllably. Consequently, it is possible to control whether there is destructive or constructive interference, and light can be modulated at very high frequency (Tb/sec). The ability to change the refractive index of a material with light, using the $\mathrm{Re}(\chi^{(3)})$ of the waveguide material, is a critical aspect of AOS. However, if there is large 2PA, two problems may arise: (1) for applications using high optical power, the carrier light may be absorbed in the waveguide, resulting in unacceptably high optical loss; and (2) the high-intensity control beam can be absorbed instead of changing the refractive index in the Mach-Zehnder arm, which can render optical modulation ineffective. An important figure of merit (FOM) for an AOS material is $|\mathrm{Re}(\chi^{(3)})/\mathrm{Im}(\chi^{(3)})|$, and this ratio needed to be greater than 12.[10] For almost all organic materials that had been examined, it was difficult to identify examples with both (1) a reasonable $|\mathrm{Re}(\chi^{(3)})|$ and (2) a sufficiently low 2PA cross section to achieve a FOM of 12 or greater. This was such a sufficiently difficult and challenging problem that companies actually stopped working on organic materials for AOS.

It is possible to achieve large $|\mathrm{Re}(\chi^{(3)})|$ and, simultaneously, a 2PA cross section sufficiently low for a FOM greater than 12. Here, we examine a simple model to optimize $|\mathrm{Re}(\chi^{(3)})|$ based on a parameter referred to as bond-length alternation (BLA). In simple donor–acceptor polymethine or polyene molecules, the extent of charge transfer from the donor to acceptor in the ground state can be related to the BLA. BLA is defined as the average of the differences in the length between adjacent carbon–carbon bonds in a polymethine $[(CH)_n]$ chain. Unsubstituted polyenes have alternating double and single bonds (bond lengths roughly 1.34 Å and 1.45 Å, respectively) and thus show a high degree of BLA (+0.11 Å). Another related parameter is the π−bond order, an electronic measure of the double-bond character of a given carbon–carbon bond. Thus, the difference in the π−bond order between adjacent carbon–carbon bonds is the bond-order alternation, where the bond order of a double bond is 2 and the bond order of a single bond is 1.[1,16]

A simplistic explanation is as follows: In polyenes, the molecule can be thought of as a linear combination of "resonance forms" in which one is neutral and one is charge-separated. If either of the forms greatly dominates the ground-state structure, the molecule will have a very large degree of BLA. When donors and acceptors are added (typically to the ends of the polyene chains), the relative contribution of the neutral and charge-separated resonance forms, and, thus, the BLA can be tuned. If these molecules are synthesized such that the donor and acceptor are strong and nearly identical in structure, both resonance forms of the molecule are equivalent in energy, and BLA goes to zero; this is the so-called "cyanine" limit, as shown in **Figure 3**.[1,11,15]

Working with Chris Gorman,[16] Jean-Luc Brédas,[1,11,15] and others, we computationally and systematically varied the polarization of these molecules, which enabled us to tune the BLA from the polyene-like form through the cyanine limit and finally to a charge-separated-like form. As a function of BLA, third-order nonlinearity was observed to start out small, become increasingly positive, become very large and negative at the cyanine limit, and then become positive again beyond the cyanine limit. It is worth noting that materials with both positive and negative $\mathrm{Re}(\chi^{(3)})$ are useful in AOS. Based on this, cyanine molecules appeared to be interesting candidates for maximizing third-order nonlinear optical properties.[6,10]

Cyanine dyes have large negative third-order nonlinearities, and these nonlinearities increase rapidly with length. They have sharp absorption bands, which mean that materials can potentially have little linear (one-photon) absorption at energies that are typically used in AOS devices.

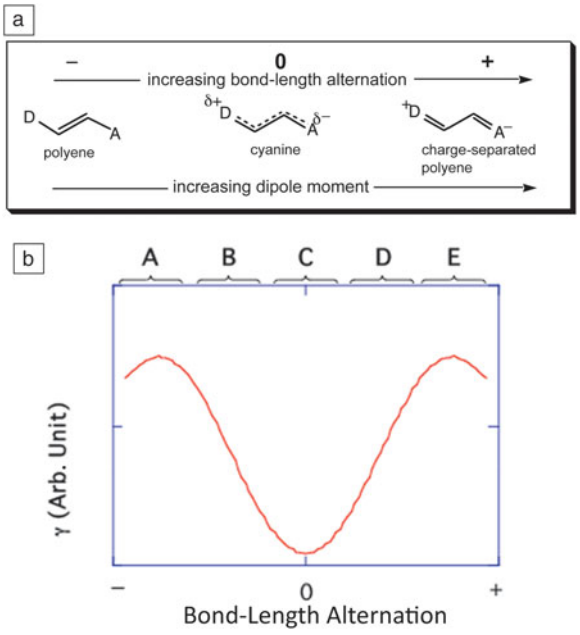


Figure 3. (a) Contribution of neutral and charge-separated resonance forms to the ground-state structure of molecules and the impact on bond-length alternation (BLA) and bond-order alternation as explained in the text and (b) variation of polarization γ plotted versus BLA for a simple donor (D)–acceptor (A) polyene. At the polyene limit (region A in the figure), γ starts small and positive, and then increases, reaching a positive peak. With further polarization, γ then (region B) decreases, (region C) changes sign, and reaches a large negative peak at the cyanine limit (bond-length alternation = 0). As the polarization further increases, γ (region D) becomes more positive and (region E) reaches a second positive peak before decreasing in value. Note: δ^+, partial positive charge; δ^-, partial negative charge.

https://doi.org/10.1557/mrs.2015.310 Published online by Cambridge University Press

Unfortunately, cyanine dyes aggregate because they are among the most polarizable molecules known, which can be problematic.[13]

Our team examined a particular cyanine dye that had a very large negative $Re(\chi^{(3)})$, but at certain input wavelengths, it unexpectedly had almost no 2PA, which is exactly what was needed for a high AOS FOM. The reasons these molecules have that particular property has to do with the spacing of excited states and the widths of electronic transitions between states.[10] Critically, cyanine molecules end up having a large spacing between one excited state and a higher excited state, such that two photons of a certain energy fall between the lower and upper excited states and are not absorbed by 2PA, leading effectively to an operational window for high FOM. With this realization, other molecules were carefully designed in which $|Re(\gamma)/Im(\gamma)|$ ranged from ca. 95 to 190, which at the time was largely unprecedented for molecules with such large $|\gamma|$.[10]

For these molecules to be useful in AOS applications, they need to be used at very high concentrations because $Re(\chi^{(3)})$ is a function of the number of molecules with a given second hyperpolarizability per unit volume (sometimes in solution, but usually in films that are at least 50% by weight of cyanine). These cyanine molecules are highly polarizable and tend to aggregate. When aggregated, additional excited states are created, which quickly become problematic. These molecules were designed to have a large energetic separation between the first and second excited states. However, aggregation leads to additional excited states that cause the absorption spectrum to change drastically and introduce new 2PA bands[11] that severely reduce the FOM, which is the case for the molecule in **Figure 4**, top left. Thus, the π-electron systems of each molecule must be prevented from interacting with neighboring molecules, even at high concentrations in the solid state.

To alleviate this, rigid groups are positioned on the molecules that would effectively prevent the molecules from aggregating (Figure 4, top right). If certain groups are placed in the middle to effectively surround the cyanine chain, the molecules can be kept from getting too close in the middle, but can interact with each other at the ends. If certain groups are positioned on the ends of the cyanine, then the cyanines can interact with each other in the middle. In order to prevent aggregation, spacer groups need to be added to both the middle and ends of the molecule. This enabled large $|Re(\chi^{(3)})|$ and low 2PA to be achieved simultaneously in highly concentrated films for a two-photon FOM greater than 12, which is the case for molecules with the substitution pattern such as that shown in Figure 4, top right. In some cases, the linear loss (largely from scattering due to inhomogeneity in the film, or to vibrational overtone absorption of the polymer matrix) reduces sufficiently to the point that waveguide devices for AOS applications can be considered.[13]

My colleagues Norwood and Peyghambarian at The University of Arizona have used these materials in solution-core optical-fiber devices.[12] When light is sent through an optical fiber, there is a process called "self-phase modulation," which takes a pulse that is very narrow in linewidth and broadens the pulse over many wavelengths as it travels through the fiber due to nonlinearities in the fiber-optic materials. Ideally, a fiber with no third-order nonlinearity would have no self-phase modulation, and thus, no broadening of the optical pulse.[12] The group took hollow-core optical fibers and filled them with a solvent that had a positive third-order nonlinearity, which had some of our molecules dissolved in it. These molecules have very large negative nonlinearity, to the point where their negative nonlinearity cancelled the positive nonlinearity of the solvent for the wavelength of the light traveling through the fiber. In this manner, they were able to cancel the self-phase modulations for a pulse traveling a reasonably long length (50 cm). The ability to do this is important for several optical-fiber-based applications that require high optical power.[12]

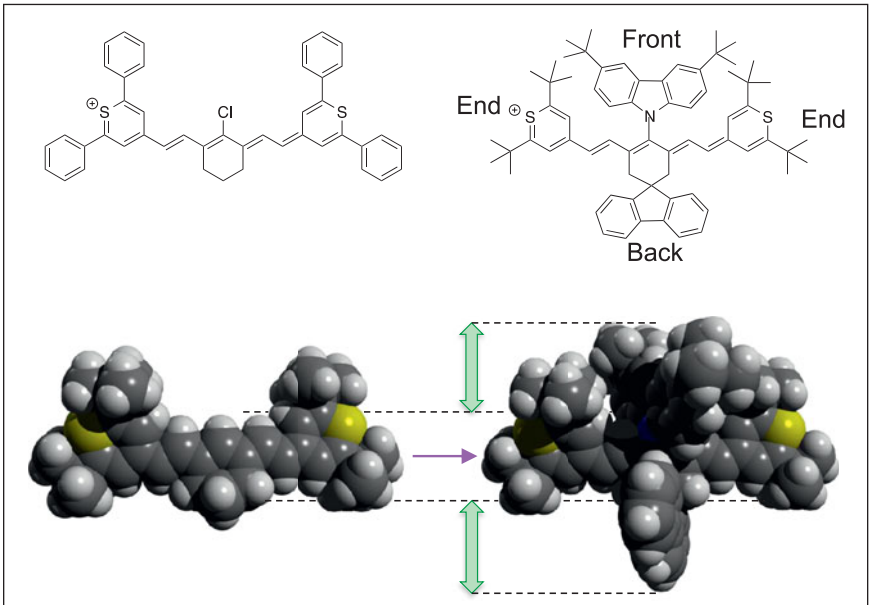


Figure 4. (Top left) An example of a positively charged cyanine dye that exhibits spectral features indicative of the formation aggregates at high concentration in solution and in neat films, and (top right) a positively charged cyanine dye with groups on the "Front," "Back," and "End," which tend to diminish close approaches of neighboring molecules in the solid state, suppressing aggregate formation. (Bottom left) Space-filling model representation of a cyanine dye without blocking groups (coloring scheme for atoms: yellow = S, light gray = H, and dark gray = C), and (bottom right) a compound with close approaches by other molecules to the conjugated core "blocked" by the groups on the "Front," "Back," and "Ends" (illustrated by the large green arrows showing the extent to which the core of the dye is "blocked"). Reproduced with permission from Reference 13. © 2014 Royal Society of Chemistry.

https://doi.org/10.1557/mrs.2015.310 Published online by Cambridge University Press

Summary

In as much as one can summarize 25 years of research with many excellent colleagues—third-order nonlinear optical properties are certainly not simple—there are real parts and imaginary parts, and these can be positive or negative. Importantly, however, they can be systematically optimized if an understanding of how the molecules can be designed is developed using a combination of first-principle quantum mechanics, some chemical intuition, and challenging synthetic work. For 2PA, donor–acceptor–donor molecules have large two-photon cross sections. Today, there are commercial two-photon 3D microfabrication systems that use two-photon microfabrication and companies that use two-photon 3D microfabrication to make products. Cyanine molecules can be very good at possessing large $|\mathrm{Re}(\chi^{(3)})|$ while having a very low 2PA at a particular wavelength, and we speculate that, through combinations of novel device designs, coupled with cyanine molecules of the type discussed previously, third-order nonlinear applications based on all-optical switching will become feasible. We are working together with other groups to realize this goal.

Acknowledgments

The research described in this article was only possible through the collaborative efforts of colleagues and their research teams and most particularly, my colleagues Joseph Perry, Jean-Luc Brédas, Steve Barlow, and Bernard Kippelen. In addition, I have worked closely with Nasser Peyghambarian, Robert Norwood, Eric Van Stryland, Alex Jen, and Larry Dalton. Most of us have worked together as a team for over 20 years on theory, synthesis, and characterization to obtain an overall picture. Our team has had numerous talented students and postdocs, who have made invaluable contributions to our understanding of second- and third-order organic nonlinear optical materials. We have had sustained support from various funding agencies (most notably, NSF, AFOSR, ONR, and DARPA), and I think that I can speak for the entire team in saying that we are very grateful to have had the chance to work together and contribute to this exciting field. In addition, I am grateful to Tim Parker and Steve Barlow for comments and suggestions on this manuscript.

References

1. F. Meyers, S.R. Marder, B.M. Pierce, J.-L. Brédas, *J. Am. Chem. Soc.* **116** (23), 10703 (1994).
2. M. Albota, D. Beljonne, J.-L. Brédas, J.E. Ehrlich, J.-Y. Fu, A.A. Heikal, S.E. Hess, T. Kogej, M.D. Levin, S.R. Marder, D. McCord-Maughon, J.W. Perry, H. Röckel, M. Rumi, G. Subramaniam, W.W. Webb, X.-L. Wu, C. Xu, *Science* **281** (5383), 1653 (1998).
3. B.H. Cumpston, S.P. Ananthavel, S. Barlow, D.L. Dyer, J.E. Ehrlich, L.L. Erskine, A.A. Heikal, S.M. Kuebler, I.-Y.S. Lee, D. McCord-Maughon, J. Qin, H. Röckel, M. Rumi, X.-L. Wu, S.R. Marder, J.W. Perry, *Nature* **398**, 51 (1999).
4. M. Rumi, J.E. Ehrlich, A.A. Heikal, J.W. Perry, S. Barlow, Z. Hu, D. McCord-Maughon, T.C. Parker, H. Röckel, S. Thayumanavan, S.R. Marder, D. Beljonne, J.-L. Brédas, *J. Am. Chem. Soc.* **122**, 9500 (2000).
5. W. Zhou, S.M. Kuebler, K.L. Braun, T. Yu, J.K. Cammack, C.K. Ober, J.W. Perry, S.R. Marder, *Science* **296**, 1106 (2002).
6. J.M. Hales, S. Zheng, S. Barlow, S.R. Marder, J.W. Perry, *J. Am. Chem. Soc.* **128** (35), 11362 (2006).
7. S.-J. Chung, S. Zheng, T. Odani, L. Beverina, J. Fu, L.A. Padilha, A. Biesso, J.M. Hales, X. Zhan, K. Schmidt, A. Ye, E. Zojer, S. Barlow, D.J. Hagan, E.W. Van Stryland, Y. Yi, Z. Shuai, G.A. Pagani, J.-L. Brédas, J.W. Perry, S.R. Marder, *J. Am. Chem. Soc.* **128** (45), 14444 (2006).
8. S.R. Marder, J.-L. Brédas, J.W. Perry, *MRS Bull.* **32** (7), 561 (2007).
9. W. Haske, V.W. Chen, J.M. Hales, W. Dong, S. Barlow, S.R. Marder, J.W. Perry, *Opt. Express* **15** (6), 3426 (2007).
10. J.M. Hales, J. Matichak, S. Barlow, S. Ohira, K. Yesudas, J.-L. Brédas, J.W. Perry, S.R. Marder, *Science* **327** (5972), 1485 (2010).
11. R.L. Gieseking, S. Mukhopadhyay, C. Risko, S.R. Marder, J.-L. Brédas, *Adv. Mater.* **26**, 68 (2014).
12. S. Shahin, K. Kieu, J.M. Hales, H. Kim, Y.A. Getmanenko, Y. Zhang, J.W. Perry, S.R. Marder, R.A. Norwood, N. Peyghambarian, *J. Opt. Soc. Am. B.* **31**, 2455 (2014).
13. S. Barlow, J.-L. Brédas, Y.A. Getmanenko, R.L. Gieseking, J.M. Hales, H. Kim, S.R. Marder, J.W. Perry, C. Risko, Y. Zhang, *Mater. Horiz.* **1**, 577 (2014).
14. Z.A. Li, T.R. Ensley, H. Hu, Y. Zhang, S.-H. Jang, S.R. Marder, D.J. Hagan, E.W. Van Stryland, A.K.-Y. Jen, *Adv. Opt. Mater.* **3**, 900 (2015).
15. J.M. Hales, S. Barlow, H. Kim, S. Mukhopadhyay, J.-L. Brédas, J.W. Perry, S.R. Marder, *Chem. Mater.* **26**, 549 (2014).
16. C.B. Gorman, S.R. Marder, *Proc. Natl. Acad. Sci. U.S.A.* **90** (23), (1993) p. 11297.
17. L. Mach, *Z. Instrumentkd.* **12**, 89 (1892).
18. L. Zehnder, *Z. Instrumentkd.* **11**, 275 (1891). □



Seth R. Marder is currently the Georgia Power Chair of Energy Efficiency and Regents' Professor of Chemistry and Materials Science and Engineering at the Georgia Institute of Technology. He is a Fellow of MRS, the American Association for the Advancement of Science, the Optical Society of America, SPIE, the Royal Society of Chemistry, and the American Physical Society. He is a recipient of the ACS Cope Scholar Award, the MRS Mid-Career Researcher Award, and an NSF Special Creativity Award. Marder can be reached by email at seth.marder@chemistry.gatech.edu.



https://doi.org/10.1557/mrs.2015.310 Published online by Cambridge University Press

MRS Communications

2015
Volume 5, Issue 4



PLASMONICS, PHOTONICS, AND METAMATERIALS PROSPECTIVE

Biosensing using photonic crystal nanolasers

Toshihiko Baba, Yokohama National University, Japan

Photonic crystal nanolasers are fabricated and operated simply, and can be applied as disposable sensors for biomedical applications. They are sensitive to the change with environmental index and surface charge. Functionalizing the nanolaser surface with an antibody, the specific binding of target antigen is detected with a detection limit 2–4 orders lower than that achieved by current standard methods, enzyme-linked immuno-sorbent assay. Nanolasers also detect negatively-charged deoxyribonucleic acid from their emission intensity. This technique requires neither labels nor spectroscopy, which simplifies screening procedures. Its applicability for high-speed detection of endotoxin and for label-fee imaging of living cells are also demonstrated. DOI: 10.1557/mrc.2015.73

PLASMONICS, PHOTONICS, AND METAMATERIALS RESEARCH LETTERS

Optical properties of high-quality nanohole arrays in gold made using soft-nanoimprint lithography

M.A. Verschuuren, Philips Research, The Netherlands; **M.J.A. de Dood** and **D. Stolwijk**, Huygens Laboratory, The Netherlands; **G.W. 't Hooft**, Philips Research and Huygens Laboratory, The Netherlands; and **A. Polman**, FOM Institute AMOLF, The Netherlands

We present a novel soft-nanoimprint procedure to fabricate high-quality sub-wavelength hole arrays in optically thick films of gold on glass substrates. We fabricate 0.5 × 0.5 mm^2 structures composed of a square array of 180 nm-diameter holes with a 780 nm pitch. Optical angular transmission measurements on the arrays show clear extraordinary transmission peaks corresponding to the dispersion of surface plasmon polaritons propagating on either side of the metal film. The transmission features can be strongly controlled by engineering the dielectric environment around the holes. As the nanoimprint procedure enables fabrication of nanoscale patterns over wafer-scale areas at low cost, these imprinted metal nanoparticle arrays can find applications in, e.g., optical components, photovoltaics, integrated optics, and microfluidics. DOI: 10.1557/mrc.2015.70

Nonlinear nanocircuitry based on quantum tunneling effects

Pai-Yen Chen, Wayne State University, USA; **Khai Q. Le**, University of Minnesota, Duluth, USA, and Hoa Sen University, Vietnam; and **Andrea Alù**, The University of Texas at Austin, USA

Metatronics, or metamaterial-inspired optical nanocircuitry, has provided a powerful toolset to tailor and implement modular quasi-static circuit functionalities in the optical regime. So far, these concepts have been mostly limited to linear operations, while many of the relevant operations in integrated circuits require nonlinear responses. In this work, we introduce nonlinear infrared nanocircuit elements exploiting large quantum conductance driven by photon-assisted tunneling and enhanced by hybrid plasmonic nanojunctions. Based on these concepts, we present infrared lumped nanocircuit mixers and switches for second-harmonic generation, and wide-spectrum self-amplitude modulators based on nanorods. DOI: 10.1557/mrc.2015.75

Self-assembly of plasmonic/excitonic silicon nanocrystals into photonic crystals

Jihua Yang, **Nicolaas J. Kramer**, **Christopher J. Hogan Jr.**, and **Uwe R. Kortshagen**, University of Minnesota, USA

In this work, photonic crystals of plasmonic/excitonic semiconductor nanocrystals (NCs) were assembled from nonthermal plasma-synthesized boron-doped silicon (Si) NCs. The photonic crystals form an inverse opal structure with larger refractive index than the conventional crystals made from silica nanoparticles and are aimed at controlling light propagation via excitonic and plasmonic absorption of the B-doped Si NC as well as the photonic band gap of the photonic crystal. Furthermore, we demonstrate self-assembly of mesoscopic photonic crystal particles consisting of B-doped Si NCs with well-defined inverse opal structure via simple aerosol processing. DOI: 10.1557/mrc.2015.77

https://doi.org/10.1557/mrs.2015.310 Published online by Cambridge University Press

Optoplasmonic networks with morphology-dependent near- and far-field responses

Wonmi Ahn, **Xin Zhao**, **Yan Hong**, and **Björn M. Reinhard**, Boston University, USA

Optoplasmonic networks consisting of dielectric microsphere resonators and plasmonic nanoantennas in a morphologically well-defined on-chip platform support unique electromagnetic signatures that are hybrids of photonic whispering gallery modes and localized surface plasmon resonances. Here we explore the dependence of their near- and far-field responses on key structural parameters, including the size of the gold nanoparticles forming the plasmonic elements, the separation between the microspheres, and the geometry of the chain. The high degree of structural flexibility, which is experimentally accessible through template guided self-assembly approaches, makes these optoplasmonic structures a unique electromagnetic material for tuning spectral shapes and intensities. DOI: 10.1557/mrc.2015.78

Surface plasmon propagation on overcrossing metallic waveguides fabricated by a pick-and-place method

Yusuke Nagasaki, **Masashi Miyata**, **Mai Higuchi**, and **Junichi Takahara**, Osaka University, Japan

Plasmonic waveguides can transport light while still confining it beyond the diffraction limit. Recently, crossing plasmonic waveguides have been suggested for the implementation of higher-density optical networks. However, suppressing undesirable scattering at their crossing point is still a challenging task because waveguides in these structures are physically connected. Here, we present an experimental demonstration of surface plasmon propagation on an overcrossing metallic waveguide fabricated by a pick-and-place method. By spatially separating the waveguides, the undesirable interaction at the interconnection can be suppressed. Our approach could be a powerful platform to achieve high-density integration of optical waveguides. DOI: 10.1557/mrc.2015.80

RESEARCH LETTERS

Mechanical properties of $APbX_3$ (A = Cs or CH_3NH_3; X = I or Br) perovskite single crystals

Yevgeny Rakita, **Sidney R. Cohen**, **Nir Klein Kedem**, **Gary Hodes**, and **David Cahen**, Weizmann Institute of Science, Israel

The remarkable optoelectronic and especially photovoltaic performance of hybrid organic–inorganic perovskite (HOIP) materials drives efforts to connect materials properties to this performance. From nano-indentation experiments on solution-grown single crystals we obtain elastic modulus and nano-hardness values of $APbX_3$ (A = Cs, CH_3NH_3; X = I, Br). The Young's moduli are ~14, 19.5, and 16 GPa, for $CH_3NH_3PbI_3$, $CH_3NH_3PbBr_3$, and $CsPbBr_3$, respectively, lending credence to theoretically calculated values. We discuss the possible relevance of our results to suggested "self-healing," ion diffusion, and ease of manufacturing. Using our results, together with literature data on elastic moduli, we classified HOIPs amongst the relevant material groups, based on their elastomechanical properties. DOI: 10.1557/mrc.2015.69

Influence of morphological disorder on in- and out-of-plane charge transport in conjugated polymer films

Anton Li, **Ban Xuan Dong** and **Peter F. Green**, University of Michigan, USA

Thin films of the conjugated polymer poly(3-hexylthiophene) (P3HT) of different morphological structures were fabricated using both conventional spin-casting and the matrix-assisted pulsed laser evaporation (MAPLE). Films deposited by MAPLE exhibit inhomogeneous morphologies comprised globular subfeatures with dimensions of the order of 100 nm. We show that whereas the in-plane carrier mobilities of MAPLE-deposited films (8.3×10^{-3} $cm^2/V/s$) are comparable with those of spin-cast analogs (5.5×10^{-3} $cm^2/V/s$), the out-of-plane mobilities are an order of magnitude lower (4.1×10^{-4} $cm^2/V/s$ versus 2.7×10^{-3} $cm^2/V/s$). Both in- and out-of-plane carrier transport characteristics of MAPLE-deposited films indicate a broad density of states and high carrier trap concentration. Optical absorbance spectroscopy not only corroborates a high degree of energetic disorder in MAPLE-deposited films, but also suggests that the P3HT chains possess average conjugation lengths comparable with spin-cast counterparts. Our findings, rationalized in terms of the Gaussian Disorder Model, describing carrier transport in an environment characterized by both positional and energetic disorder, provide important perspectives on the extent to which disorder impacts mechanisms of charge transport in conjugated polymers. DOI: 10.1557/mrc.2015.72

Indacenodithiophene-benzothiadiazole organic field-effect transistors with gravure-printed semiconductor and dielectric on plastic

Stuart G. Higgins, **Beinn V.O. Muir**, **Martin Heeney**, and **Alasdair J. Campbell**, Imperial College London, UK

We demonstrate the gravure printing of a high-performance indacenodithiophene (IDT) copolymer, indacenodithiophene–benzothiadiazole (C16IDT–BT), onto self-aligned organic field-effect transistor architectures on flexible plastic substrates. We observed that the combination of a gravure-printed dielectric with gravure-printed semiconductor yielded devices with higher mean-effective mobility than devices manufactured using photolithographically patterned dielectric. Peak mobilities of μ = 0.1 cm^2 V^{-1} s^{-1} were measured, and exceed previous reports for non-printed C16IDT-BT on non-flexible silicon substrates. DOI: 10.1557/mrc.2015.66

https://doi.org/10.1557/mrs.2015.310 Published online by Cambridge University Press

Ultrahigh strength of 3D printed diluted magnesium doping wollastonite porous scaffolds

Jiajun Xie, **Huifeng Shao**, **Dongshuang He**, **Xianyan Yang**, **Chunlei Yao**, **Juan Ye**, **Yong He**, **Jianzhong Fu**, and **Zhongru Gou**, Zhejiang University, China

Beyond the traditional phase conversion or biphase mixing hybrid, we developed the dilute magnesium-doped wollastonite inks and three-dimensional (3D) printing approaches to fabricate the ultrahigh strength bioceramic porous scaffolds. The mechanical strength (>120 MPa) of the porous bioceramics was an order of magnitude higher than the pure wollastonite and other stoichiometric Ca-Mg silicate porous bioceramics. This abnormal but expected improvement in strength in bioceramic scaffolds is equivalent or even superior to the mechanical requirement in load bearing bone defects. The breakthrough is totally unexpected, and it quickly opens the door for the 3D printing bioceramics manufacture and large-area segmental bone defect repair applications. DOI: 10.1557/mrc.2015.74

Evidence of electric-field-accelerated growth of tin whiskers

Anthony C. Vasko and **Corey R. Grice**, University of Toledo, USA; **Andrew D. Kostic**, Aerospace Corporation, USA; and **Victor G. Karpov**, University of Toledo, USA

This paper presents experimental results supporting a theory that electric fields accelerate the growth of tin (Sn) whiskers. We have rapidly (within one week) grown long (~100 μm) and dense (~300 mm^{-2}) whiskers on thin Sn films. Humidity and an applied electric field are found to have a strong effect when applied together, making whiskers orders of magnitude longer and denser. An evidence of explosive whisker development is presented. DOI:10.1557/mrc.2015.64

A correction method of elastic modulus in compression tests for linear hardening materials

Wei Liu, **Yong Huan**, **Jie Dong**, **Yujing Dai Yujing**, and **Ding Lan**, Chinese Academy of Sciences, China

A correction method for linear hardening materials is brought forward to obtain the true (or nearly true) modulus of cylinder specimens with middle aspect ratios in compression tests. By considering the stress concentration near the interface between the specimen and the compression platen caused by slant contact, a “sandwich” model is developed. A correction formula is derived and all parameters can be obtained from the tested stress-strain curve. Experiments were performed on Al 2024 specimens with four aspect ratios. The corrected results are closer to the intrinsic modulus than the tested values, which verify the effectiveness of the correction method. DOI: 10.1557/mrc.2015.76

Toward anti-fouling capacitive deionization by using visible-light reduced TiO_2/graphene nanocomposites

Wei Zhang, University of South Australia, Australia and **Baoping Jia**, Changzhou University, China

In this work, we showcased a visible-light-assisted reduction of graphene oxide (GO) using N-doped TiO_2 photocatalysts. Bench scale capacitive deionization (CDI) experiments determine the optimum working voltage for TiO_2–reduced graphene oxide (RGO) nanocomposites as CDI electrodes at 1.8 V. Furthermore, the coupled TiO2nanoparticles within the as-prepared composite also exhibited photocatalytic ability by removing the humic acid model pollutant. This property is expected to be beneficial as it could relieve the degree of fouling on the electrosorptive surface caused by dissolved organic compounds. In the end, we have demonstrated their potential as a viable desalination water treatment technology in a pilot scale CDI unit. DOI: 10.1557/mrc.2015.65

Reduced-temperature solution-processed transparent oxide low-voltage-operable field-effect transistors

Yu Liu, Johns Hopkins University, USA; **Kyle McElhinny**, University of Wisconsin–Madison, USA; **Olivia Alley**, Johns Hopkins University, USA; **Paul G. Evans**, University of Wisconsin–Madison, USA; and **Howard E. Katz**, Johns Hopkins University, USA

Metal oxide-based transistors can be fabricated by low-cost, large-area solution processing methods, but involve a trade-off between low processing temperature, facile charge transport and high-capacitance/low-voltage transistor gates. We achieve these simultaneously by fabricating ZnO and sodium-incorporated alumina (SA) thin films with temperature not exceeding 200 to 250 °C using aqueous and combustion precursors, respectively. X-ray reflectivity shows a compositionally distinct SA boundary layer forming near the substrate and that a portion of the SA is chemically removed during the subsequent semiconductor deposition. Improved etch resistance and reduced dielectric leakage was obtained when (3-glycidoxypropyl) trimethoxysilane was included in the SA precursor. DOI: 10.1557/mrc.2015.79

For more information or to submit your manuscript for review, visit:
www.mrs.org/mrc.

https://doi.org/10.1557/mrc.2015.310 Published online by Cambridge University Press

INTRODUCING...

MRS Advances

A NEW PEER-REVIEWED ONLINE-ONLY JOURNAL

from the Materials Research Society and Cambridge University Press

- devoted to publishing new and emerging materials science
- designed to reflect the way materials researchers work, write, publish and share their results
- editorial leadership ensures rapid peer review and speed of publication
- immediate global distribution alongside the MRS portfolio of world-class, peer-reviewed publications
- FREE to all MRS members

Inaugural Content Now Available!

mrs.org/mrs-advances



MRS MATERIALS RESEARCH SOCIETY | CAMBRIDGE UNIVERSITY PRESS

https://doi.org/10.1557/adv.2015.31 Published online by Cambridge University Press